

# Conduction and Valence Band Positions of Ta<sub>2</sub>O<sub>5</sub>, TaON, and Ta<sub>3</sub>N<sub>5</sub> by UPS and Electrochemical Methods

Wang-Jae Chun,<sup>†,‡</sup> Akio Ishikawa,<sup>†</sup> Hideki Fujisawa,<sup>§</sup> Tsuyoshi Takata,<sup>†</sup> Junko N. Kondo,<sup>†</sup> Michikazu Hara,<sup>†</sup> Maki Kawai,<sup>§</sup> Yasumichi Matsumoto,<sup>||</sup> and Kazunari Domen<sup>\*,†,‡,⊥</sup>

Chemical Resources Laboratory, Tokyo Institute of Technology, 4259 Nagatsuta, Midori-ku, Yokohama 226-8503, Japan, Catalysis Research Center Hokkaido University Sapporo 060-0811, Japan, Surface Chemistry Laboratory, Institute of Physical and Chemical Research (RIKEN), 2-1 Hirosawa, Wako 351-0198, Japan, Department of Applied Chemistry, Faculty of Engineering, Kumamoto University, 2-39-1 Kurokami, Kumamoto 860-0862, Japan, and Core Research for Evolutional Science and Technology (CREST), Japan Science and Technology Co. (JST)

Received: December 2, 2002

The conduction and valence band edges for electronic band gaps and Fermi levels are determined for Ta<sub>2</sub>O<sub>5</sub>, TaON, and Ta<sub>3</sub>N<sub>5</sub> by ultraviolet photoelectron spectroscopy (UPS) and electrochemical analyses. Reasonable agreement between the results of the two methods is obtained at the pH at which the  $\zeta$  potentials of the particles are zero. The tops of the valence bands are found to be shifted to higher potential energies on the order Ta<sub>2</sub>O<sub>5</sub> < TaON < Ta<sub>3</sub>N<sub>5</sub>, whereas the bottoms of the conduction bands are very similar in the range −0.3 to −0.5 V (vs NHE at pH = 0). From the results, it is concluded that TaON and Ta<sub>3</sub>N<sub>5</sub> are promising catalysts for the reduction and oxidation of water using visible light in the ranges  $\lambda < 520$  nm and  $\lambda < 600$  nm, respectively. It is also demonstrated that the proposed UPS technique is a reliable alternative to electrochemical analyses for determining the absolute band gap positions for materials in aqueous solutions that would otherwise be difficult to measure using electrochemical methods.

## 1. Introduction

For most photoelectronic applications of semiconductors and insulators, the knowledge of absolute band gap positions is essential. The present authors have been investigating the utilization of various oxides and non-oxide materials as photocatalysts for overall water splitting in an effort to achieve efficient photochemical energy conversion.<sup>1–3</sup> The thermodynamic requirements for solid-state photocatalysts suitable for overall water splitting are as follows.

The bottom of the conduction band  $E_{CB}$  should be more negative than the H<sup>+</sup>/H<sub>2</sub> redox potential, that is, 0 V vs NHE at pH = 0 (or the electron potential should be more positive than −4.44 eV vs the vacuum level).

The top of the valence band  $E_{VB}$  should be more positive than the O<sub>2</sub>/OH<sup>−</sup> redox potential, that is, +1.23 V vs NHE at pH = 0 (or more negative than −5.6 eV vs the vacuum level).

At present, the authors are concentrating on developing promising materials for overall water splitting under visible light irradiation (400 nm <  $\lambda$  < 800 nm). A number of oxynitrides of early transition metals such as Ti<sup>4</sup> and Ta<sup>5,6</sup> have been found to be potential candidates for this application. However, the band gap positions of these materials are unknown, and in most cases the fabrication of suitable electrodes has been unsuccessful due

to difficulties in processing the powder samples. Therefore, the authors have begun to use photoelectron spectroscopy, and ultraviolet photoelectron spectroscopy (UPS) in particular, to determine the band gap positions of these materials. This method is a useful technique for this situation because the correlation between the photoelectrode potential and the absolute potential of electrons has already been established.<sup>7</sup> The sole difficulty in performing UPS measurements for such wide band gap and low-conductivity materials is undesirable charging of the samples during measurement.

In this study, Ta<sub>2</sub>O<sub>5</sub>, TaON, and Ta<sub>3</sub>N<sub>5</sub> samples prepared by several methods are analyzed by electrochemical methods and UPS to determine the band gap positions and to confirm the validity of UPS analysis for this purpose.

## 2. Experimental Section

**2.1. Sample Preparation.** Two different series of samples were prepared. One series was prepared from Ta foil for analysis by electrochemical methods and UPS. The Ta foil (10 × 10 × 0.2 mm<sup>3</sup>, 99%, Nilaco Co.) was oxidized at 823 K in air for 30 min to give a Ta<sub>2</sub>O<sub>5</sub>/Ta sample, and a Ta<sub>3</sub>N<sub>5</sub>/Ta sample was obtained by exposing a Ta<sub>2</sub>O<sub>5</sub>/Ta foil sample to NH<sub>3</sub> at 1123 K and a flow rate of 20 mL/min for 4 h. The authors also attempted to prepare TaON/Ta; however, the surface layer peeled off easily for all samples and a suitable preparation condition was not found. The second series was prepared from powder samples. TaON and Ta<sub>3</sub>N<sub>5</sub> powders were synthesized by the following procedures according to the literature.<sup>8</sup> Bright yellow TaON was obtained by exposing Ta<sub>2</sub>O<sub>5</sub> (99%, Rare Metallic Co., Ltd.) to NH<sub>3</sub> (99.999%, Mitsui Chemicals Co. Ltd.) at 1023 K and a flow rate of 20 mL/min for 20 h. Pure wine-red Ta<sub>3</sub>N<sub>5</sub> was prepared by a similar method at 1123 K

\* To whom correspondence should be addressed. E-mail: kdomen@res.titech.ac.jp.

<sup>†</sup> Chemical Resources Laboratory, Tokyo Institute of Technology.

<sup>‡</sup> Catalysis Research Center Hokkaido University.

<sup>§</sup> Surface Chemistry Laboratory, Institute of Physical and Chemical Research (RIKEN).

<sup>||</sup> Department of Applied Chemistry, Faculty of Engineering, Kumamoto University.

<sup>⊥</sup> CREST, JST.

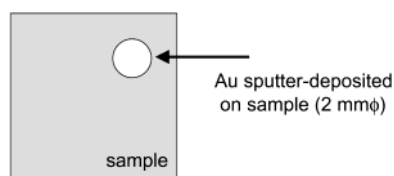


**Figure 1.** Schematic illustration of sample coated with Au.

and a flow rate of 1000 mL/min for 10–15 h. Initially, powder samples pressed into disks were employed for UPS measurement; however, reliable and reproducible data could not be obtained due mainly to sample charging. Therefore, samples were prepared by electrophoretic deposition on Pt foils.<sup>9,10</sup> TaON or Ta<sub>3</sub>N<sub>5</sub> powder (50 mg) was suspended in 50 mL of acetone containing 10 mg of I<sub>2</sub> by ultrasonication. The electrophoretic deposition of TaON or Ta<sub>3</sub>N<sub>5</sub> was performed using a thin Pt foil (25 × 10 × 0.1 mm<sup>3</sup>) as an anode. Deposition was carried out for 1 min at 20 V. The prepared sample was then washed thoroughly with acetone prior to UPS measurement.

**2.2. Characterization.** Samples were characterized by atomic force microscopy (AFM; TMX-2100, TopoMetrix), X-ray diffractometry (XRD; Geigerflex Rad-B system Cu Kα 15 mA, Rigaku), field-emission scanning electron microscopy (FE-SEM; S-4700, Hitachi) and UV–visible diffuse reflectance spectroscopy (UV–vis DR; V-560, JASCO). X-ray photoelectron spectroscopy (XPS) was performed using a VG-ADES 400 instrument (Vacuum Generators Co.) with Mg Kα X-ray source at a residual gas pressure of below 10<sup>−8</sup> Pa. The binding energy was calibrated against Au 4f<sub>7/2</sub> (83.9 eV).

**2.3. Electrochemical Measurement.** A Cu wire was attached to the Ta<sub>2</sub>O<sub>5</sub>/Ta or Ta<sub>3</sub>N<sub>5</sub>/Ta foil with silver paste, and all samples were waterproofed, except for the front surface, with epoxy resin to prevent current leakage. A Pyrex electrolytic cell was employed, filled with 20 mL of Ar-purged 0.5 M K<sub>2</sub>SO<sub>4</sub>. The pH of the solution was adjusted with 0.1 M NaOH and 0.1 M H<sub>2</sub>SO<sub>4</sub>. A Pt wire and Ag/AgCl electrode were employed as the counter and reference electrodes, respectively. Impedance measurements were recorded using a frequency response analyzer (Hz-3000, Hokuto, Ltd.).

**2.4. UPS Measurement.** UPS spectra were measured using He I excitation (21.2 eV) and recorded with a constant pass energy of 5 eV in the ultrahigh vacuum (UHV) chamber of the XPS instrument. UPS binding energies were referenced to the Fermi edge of Au, which was sputtered onto the sample in the UPS chamber. Figure 1 shows an illustration of a foil coated with Au. The spot diameters of the deposited Au and UV light were 2 mm. None of the samples were damaged in these measurements. Prior to XPS and UPS measurements, the Ta<sub>2</sub>O<sub>5</sub>/Ta sample was oxidized at 823 K for 30 min in the UHV chamber in an O<sub>2</sub> (99.999% purity) atmosphere at 5 × 10<sup>−3</sup> Pa to remove surface impurities. To maintain the purity of O<sub>2</sub> in the UHV chamber, the chamber was evacuated to 10<sup>−5</sup> Pa and charged with fresh O<sub>2</sub> every 5 min. The TaON/Pt, Ta<sub>3</sub>N<sub>5</sub>/Ta, and Ta<sub>3</sub>N<sub>5</sub>/Pt samples were subjected to low-temperature H<sub>2</sub> treatment to remove surface contamination. The samples were heated for 1 h at 523 K in the UHV chamber in an H<sub>2</sub> (99.999% purity) atmosphere at 5 × 10<sup>−3</sup> Pa. Fresh H<sub>2</sub> was introduced every 10 min.

**2.5. Measurement of ζ Potential.** The ζ potential was measured on a DELSA 440SX (Coulter). The suspension fluid was a 0.01 M aqueous solution of KCl with pH adjusted by the addition of 0.01 M HCl and 0.01 M KOH solutions.

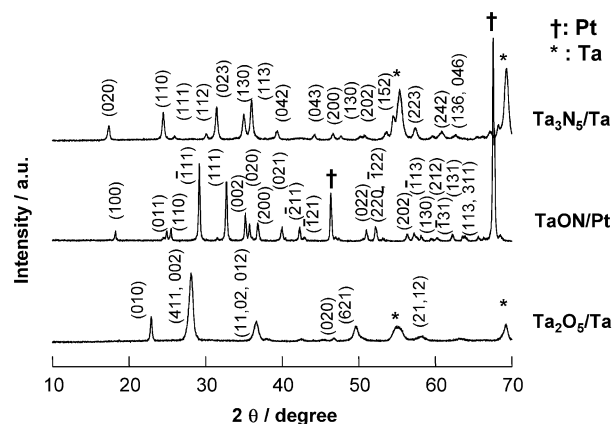


**Figure 2.** X-ray diffraction patterns of Ta<sub>2</sub>O<sub>5</sub>/Ta, TaON/Pt, and Ta<sub>3</sub>N<sub>5</sub>/Ta.

### 3. Results

**3.1. XRD, SEM, AFM, and UV–Vis DRS.** XRD patterns of Ta<sub>2</sub>O<sub>5</sub>/Ta, TaON/Pt and Ta<sub>3</sub>N<sub>5</sub>/Ta are shown in Figure 2. All diffraction peaks were assigned to Ta<sub>2</sub>O<sub>5</sub>, TaON, and Ta<sub>3</sub>N<sub>5</sub>, respectively, in addition to the substrate materials.<sup>11,12</sup> No impurity phases were observed.

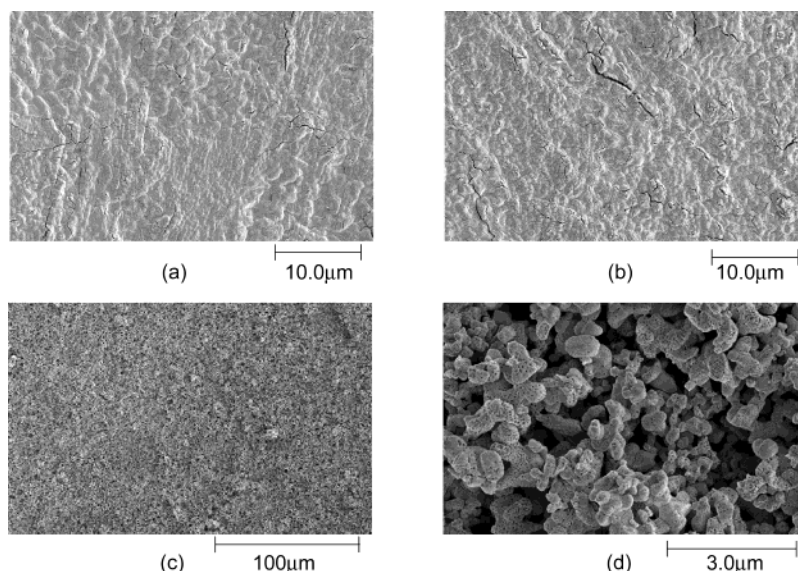
Figure 3 shows SEM images of Ta<sub>2</sub>O<sub>5</sub>/Ta, Ta<sub>3</sub>N<sub>5</sub>/Ta, and TaON/Pt. The surfaces of Ta<sub>2</sub>O<sub>5</sub>/Ta (a) and Ta<sub>3</sub>N<sub>5</sub>/Ta (b) were essentially flat, with several cracks. TaON particles electrophoretically deposited on Pt were estimated to be 0.5–1.0 μm in diameter, and the Pt substrate surface could not be observed, as shown in Figure 3c,d.

Figure 4 shows the AFM image of the TaON/Pt sample. The dark (lower) part of the image is a bare Pt area where TaON deposition was prevented. From the difference in height between the bare and coated Pt areas, the thickness of the TaON film was estimated to be about 2 μm.

Figure 5 shows the UV–vis DR spectra for powder samples of Ta<sub>2</sub>O<sub>5</sub>, TaON, and Ta<sub>3</sub>N<sub>5</sub>. TaON/Pt was prepared from TaON powder by electrophoretic deposition. The Ta<sub>3</sub>N<sub>5</sub>/Pt sample was also prepared by electrophoretic deposition with Ta<sub>3</sub>N<sub>5</sub> powder. The spectra of TaON/Pt and Ta<sub>3</sub>N<sub>5</sub>/Pt should be the same with the powder samples. The values of E<sub>BG</sub> were, therefore, determined by UV–vis DR spectra for powder samples in this paper. In the UV–vis spectra, the absorption band edges of TaON and Ta<sub>3</sub>N<sub>5</sub> occur at 520 and 600 nm, respectively, and are shifted by about 200 and 280 nm from that of Ta<sub>2</sub>O<sub>5</sub>. The band gap energies (E<sub>BG</sub>) of Ta<sub>2</sub>O<sub>5</sub>, TaON and Ta<sub>3</sub>N<sub>5</sub> were estimated to be 3.9, 2.4, and 2.1 eV, respectively.

**3.2. XPS Analysis.** XPS was used to examine the surface composition of Ta, N, and O and the oxidation state of Ta in the samples. Figure 6 shows the O1s, N1s, and Ta4f spectra of Ta<sub>2</sub>O<sub>5</sub>/Ta, TaON/Pt and Ta<sub>3</sub>N<sub>5</sub>/Ta, respectively. Peak positions are summarized in Table 1. Sample charging was often observed for the oxide powders, but was not observed for the thin-film samples including TaON/Pt. The peak positions of the O1s spectra were very similar in all samples. The observed O1s spectrum of Ta<sub>3</sub>N<sub>5</sub>/Ta most likely contains information from the area outside the sample. The spot size of the irradiated X-ray is much larger than the He I used for the UPS measurement, which is 2 mm in diameter. Judging from actual intensity, the contribution of the surface oxygen on Ta<sub>3</sub>N<sub>5</sub>/Ta should be negligibly small for UPS measurement.

No Ta<sup>0</sup> or Pt<sup>0</sup> metal peak was observed in any of the samples, indicating that the substrate was completely obscured. In Ta<sub>2</sub>O<sub>5</sub>/Ta, Ta 4f<sub>7/2</sub>, and Ta 4f<sub>5/2</sub> peaks appeared at 26.6 and 28.5 eV, respectively. These energy values correspond to Ta<sup>5+</sup> in Ta<sub>2</sub>O<sub>5</sub>



**Figure 3.** SEM image of (a)Ta<sub>2</sub>O<sub>5</sub>/Ta, (b)Ta<sub>3</sub>N<sub>5</sub>/Ta, and (c,d)TaON/Pt.

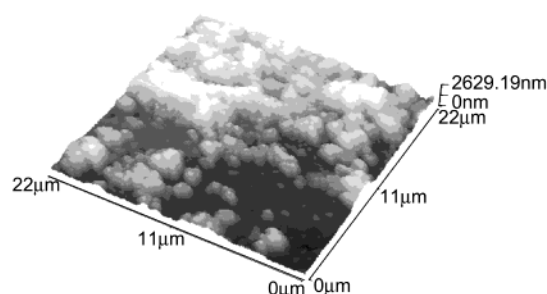


**Figure 4.** AFM image of TaON/Pt.

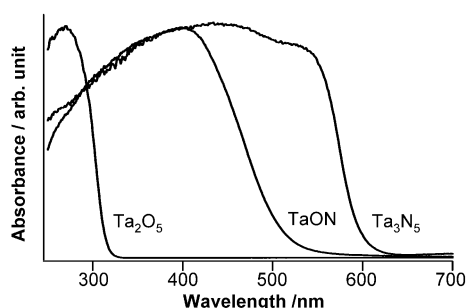


**Figure 5.** U-vis diffuse reflectance spectra of Ta<sub>2</sub>O<sub>5</sub>, TaON, and Ta<sub>3</sub>N<sub>5</sub>.

**TABLE 1: Binding Energies of O 1s, N 1s, Ta 4f<sub>5/2</sub>, and Ta 4f<sub>7/2</sub> Peaks for Ta<sub>2</sub>O<sub>5</sub>/Ta, TaON/Pt, and Ta<sub>3</sub>N<sub>5</sub>/Ta**

electrodes	O 1S/eV	N 1S/eV	Ta 4f <sub>5/2</sub> /eV	Ta 4f <sub>7/2</sub> /eV
Ta metal	N/A	N/A	23.7	21.8
Ta <sub>2</sub> O <sub>5</sub> /Ta	530.9	N/A	28.5	26.6
TaON/Pt	530.8	397.1	27.7	25.8
Ta <sub>3</sub> N <sub>5</sub> /Ta	530.7	396.5	26.7	24.8

as reported in the literature.<sup>13</sup> Ta4f peaks for TaON/Pt and Ta<sub>3</sub>N<sub>5</sub>/Ta are shifted to lower binding energies by ca. 0.8 and 1.8 eV compared to those of Ta<sub>2</sub>O<sub>5</sub>. Considering the difference in electronegativity between O and N, it is considered that the electron density around Ta atom increases with the N/O ratio. In other words, the covalency between Ta and N is greater than between Ta and O. This kind of difference could affect the band gap positions of these materials.

**3.3. Electrochemical Measurements.** To estimate flat band potentials ( $E_{FB}$ ), plots of (differential capacitance)<sup>-2</sup> against

electrode potential (Mott–Schottky plots) under different pH conditions for both electrodes were constructed, as shown in Figure 7. It was found that the flat band potential of Ta<sub>2</sub>O<sub>5</sub> depends almost linearly on the pH of the electrolyte solution with a slope of ca. -60 mV/ΔpH as seen in Figure 7a. It is known that oxide semiconductors in general react with H<sup>+</sup> or OH<sup>-</sup> ions in solution, and the band edges at the interface consequently shift with the pH of the solution by 60 mV per pH unit change in the solution. Interestingly, it was also found that the  $E_{FB}$  of Ta<sub>3</sub>N<sub>5</sub> varies linearly with pH, as seen in Figure 7b. Huygens reported that the  $E_{FB}$  of GaN is also a linear function of pH.<sup>14</sup> The  $E_{FB}$  of Ta<sub>2</sub>O<sub>5</sub> is approximately -1.3 V vs Ag/AgCl (-1.1 V vs NHE) at pH = 13 and -0.5 V vs Ag/AgCl at pH = 0 (-0.3 V vs NHE), and the  $E_{FB}$  of Ta<sub>3</sub>N<sub>5</sub> is approximately -1.0 V vs Ag/AgCl (-0.8 V vs NHE) at pH = 13 and -0.3 V vs Ag/AgCl at pH = 0 (0.0 V vs NHE). Impedance measurements could not be completed for the TaON/Pt electrode because the electrolyte penetrated down to the Pt substrate.

**3.4. UPS Measurement.** As an example, UPS spectra of TaON/Pt measured at various sample biases (0, -10, and -15 V) are shown in Figure 8. The cutoff of the UPS spectrum (or low kinetic energy region) with the sample bias of 0 V cannot be observed clearly. The cutoff position ( $E_K = 0$  eV) needs to be identified to estimate the vacuum level, and sample biases higher than the work function allow this to be achieved. At -10 and -15 V, clear cutoffs could be observed in the UPS spectra, as shown in Figure 8. The following equation should then hold:

$$E_B + E_K + \phi_{\text{analyzer}} = 21.2 \text{ eV} \quad (1)$$

where  $E_B$ ,  $E_K$  and  $\phi_{\text{analyzer}}$  are the binding energy measured from the Fermi level, the kinetic energy of the electron, and the work function of the analyzer. Therefore,  $\phi_{\text{analyzer}}$  was found to be smaller than 10 eV, and an applied potential of 10 eV was sufficient to capture the entire spectrum.

Features in the valence band and the entire spectrum remained unchanged with respect to the different biases, although the background attributed to secondary electron emission was reduced. It should be noted that none of the samples charged up during UPS measurement as in the case for XPS measurement. Figure 9 shows the UPS spectra of TaON/Pt and Au on TaON/Pt. The Fermi level of Au on TaON/Pt was estimated to



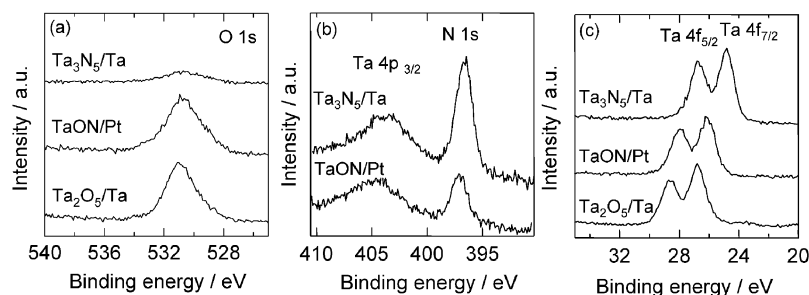


Figure 6. X-ray photoelectron spectra of Ta<sub>2</sub>O<sub>5</sub>/Ta, TaON/Pt, and Ta<sub>3</sub>N<sub>5</sub>/Ta: (a) O1s, (b) N1s, and (c) Ta4f regions.

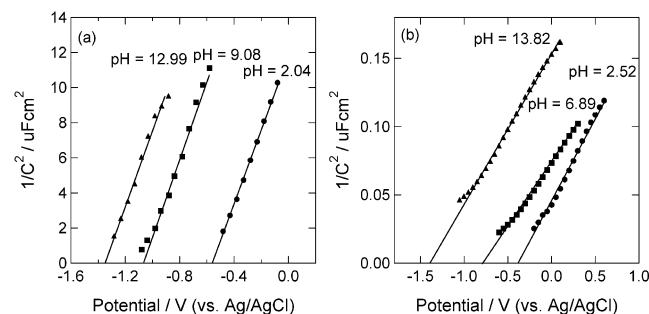


Figure 7. Mott-Schottky plots of (a) Ta<sub>2</sub>O<sub>5</sub> and (b) Ta<sub>3</sub>N<sub>5</sub> under various pH conditions.

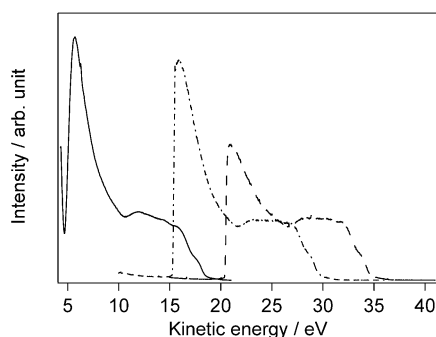


Figure 8. UPS spectra of TaON/Pt measured at various sample biases. Solid line: 5 V. Dash-dotted line: 10 V. Dashed line: 15 V.

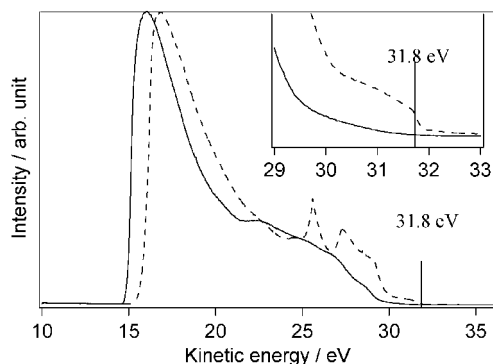


Figure 9. UPS spectra of TaON/Pt (solid line) and Au on TaON/Pt (dashed line).

be at  $E_K = 31.8$  eV in the spectrum. The Fermi level of TaON/Pt is at the same position as that of Au deposited on TaON/Pt, which allows the Fermi level to be determined experimentally.

The relationship between several energy levels ( $E_{VB}$ ,  $E_F$ , and  $E_{vac}$ ) and the UPS spectrum of TaON/Pt and Au is shown in Figure 10. The figure shows the scale of binding energy with the Fermi level of Au set at 0 V. The vacuum level ( $E_{vac}$ ) should be located 21.2 eV above the cutoff energy of the spectrum. The work functions of TaON and Au based on this definition are estimated to be 4.4 and 5.1 eV, respectively. The work

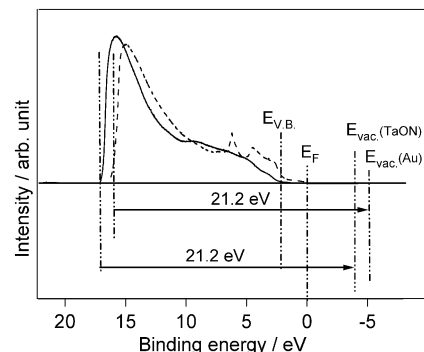


Figure 10. Comparison and relationship of  $E_{VB}$ ,  $E_F$ , and  $E_{vac}$  of UPS spectra. Solid line: TaON/Pt. Dashed line: Au on TaON/Pt.

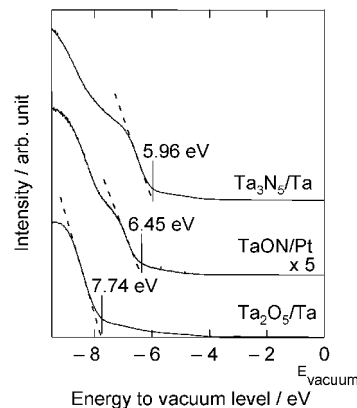
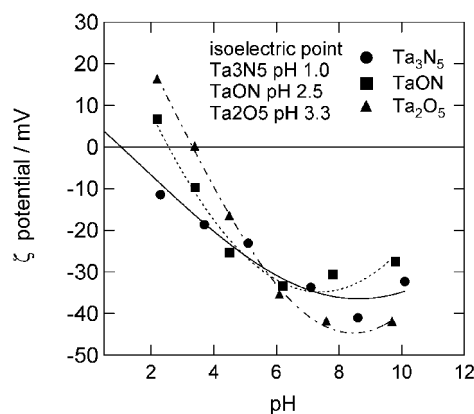


Figure 11. UPS spectra of Ta<sub>2</sub>O<sub>5</sub>/Ta, TaON/Pt, and Ta<sub>3</sub>N<sub>5</sub>/Ta in the valence band region.

function of Au is in good agreement with the literature,<sup>15</sup> and the estimated work functions of Au on Ta<sub>2</sub>O<sub>5</sub>/Ta and Ta<sub>3</sub>N<sub>5</sub>/Ta are the same as that of Au alone. Figure 11 shows a series of UPS spectra for Ta<sub>2</sub>O<sub>5</sub>/Ta, Ta<sub>3</sub>N<sub>5</sub>/Ta, and TaON/Pt in the valence band region. Ta<sub>3</sub>N<sub>5</sub>/Pt sample was prepared by electrophoretic deposition with Ta<sub>3</sub>N<sub>5</sub> powder and the UPS result was coincided with the result of Ta<sub>3</sub>N<sub>5</sub>/Ta. (UPS spectrum of Ta<sub>3</sub>N<sub>5</sub>/Pt is not shown.) In this figure, the three spectra were compared with  $E_{vac}$  at the same position. The position of the top of the valence band ( $E_{VB}$ ) for each sample is indicated on the spectrum. The  $E_{VB}$  positions in all measurements based on linear extrapolation are shown in Figure 11.  $E_{VB}$  shifts to lower binding energies with increasing nitrogen content in the sample. The  $E_{VB}$  and Fermi level for each sample are summarized in Table 2.

**3.5. Measurement of  $\zeta$  Potential.** To correlate the data obtained by the two methods, the  $\zeta$  potential was measured to determine the isoelectric point of each sample. The  $\zeta$  potential curves against pH are shown in Figure 12. The isoelectric points of Ta<sub>2</sub>O<sub>5</sub> and TaON thus determined occur at pH values of 3.3 and 2.5, respectively. For Ta<sub>3</sub>N<sub>5</sub>, the isoelectric point was



**Figure 12.**  $\zeta$  potential vs pH curves for  $\text{Ta}_2\text{O}_5$ , TaON, and  $\text{Ta}_3\text{N}_5$ .

**TABLE 2: Band Energy of  $\text{Ta}_2\text{O}_5/\text{Ta}$ , TaON/Pt, and  $\text{Ta}_3\text{N}_5/\text{Ta}$  by UPS**

electrodes	Fermi level/eV	$E_{\text{VB}}/\text{eV}$
$\text{Ta}_2\text{O}_5/\text{Ta}$	-4.25	-7.74
TaON/Pt	-4.26	-6.45
$\text{Ta}_3\text{N}_5/\text{Ta}$	-4.15	-5.96

estimated to occur at a pH of about 1.0 by extrapolation of the  $\zeta$  potential curve.

#### 4. Discussion

The relationship between the absolute electron potential of an electrode ( $E_{\text{abs}}$ ) and the standard electrode potential ( $E^\circ$ ) is expressed as follows.

$$E_{\text{abs}} = -E^\circ - 4.44 \quad (\text{at } 298 \text{ K}) \quad (2)$$

where the electron energy is 0 eV in a vacuum. This equation appears to allow correlation of the data obtained by the two methods. However, there is still uncertainty in terms of the pH to which the data obtained by UPS should be correlated. Generally, in an aqueous solution, the potential energies such as  $E_{\text{CB}}$ ,  $E_{\text{VB}}$  and  $E_{\text{F}}$ , vary depending on the pH, particularly for oxide semiconductors. This is due to surface ionization driven by adsorbed species (e.g.,  $\text{H}^+$  and  $\text{OH}^-$ ). It is considered that the net charge of the sample in UHV is zero. Therefore, the energy levels determined by UPS are assumed to correspond to those obtained in an electrolyte at the pH at which the surface charge of the sample is zero. The pH of the isoelectric points of the samples in aqueous solution was determined by measurement of the  $\zeta$  potential. From Mott-Schottky plots, the  $E_{\text{FB}}$  of  $\text{Ta}_2\text{O}_5$  and  $\text{Ta}_3\text{N}_5$  was found to shift with pH of the solution by  $-60$  mV per pH unit change. The  $E_{\text{FB}}$  of TaON is also expected to be a linear function of pH because the surface of TaON should behave similarly to the surfaces of  $\text{Ta}_2\text{O}_5$  and  $\text{Ta}_3\text{N}_5$ .

On the basis of the relationship discussed above, Figure 13 illustrates the comparison of band positions determined by UPS and electrochemical measurements at pH = 0. Table 3 lists the values of  $E_{\text{BG}}$ ,  $E_{\text{F}}$ ,  $E_{\text{VB}}$ , and  $E_{\text{CB}}$  determined by UV-vis diffuse reflectance spectra, electrochemical analysis and UPS measurements. The UPS result of  $\text{Ta}_3\text{N}_5/\text{Ta}$  was coincided with the result of  $\text{Ta}_3\text{N}_5/\text{Pt}$  sample.  $\text{Ta}_3\text{N}_5$  prepared on Ta and  $\text{Ta}_3\text{N}_5$  powder should have the same UV-vis DR spectra. The value of  $E_{\text{BG}}$  was, therefore, determined by UV-vis DR spectra for  $\text{Ta}_3\text{N}_5$  powder. It is generally known that the  $E_{\text{CB}}$  of many n-type semiconductors is 0.1–0.3 eV more negative than  $E_{\text{F}}$ .<sup>16,17</sup> On the basis of this, the difference is assumed to be  $-0.3$  eV for the determination of the band positions of  $\text{Ta}_2\text{O}_5$  and  $\text{Ta}_3\text{N}_5$  by electrochemical measurements. The band positions determined

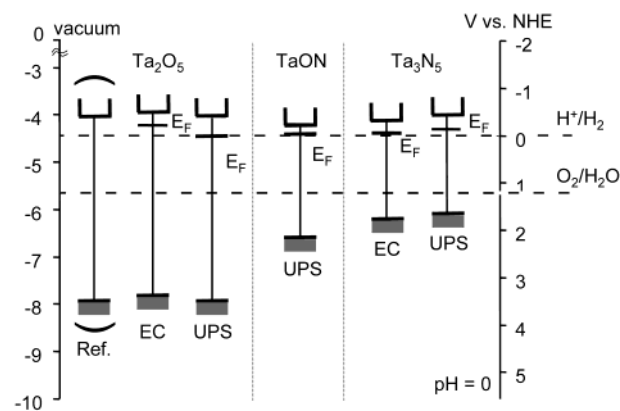


**Figure 13.** Band positions of  $\text{Ta}_2\text{O}_5$ , TaON, and  $\text{Ta}_3\text{N}_5$  determined by electrochemical analysis and UPS measurements.

**TABLE 3: Band Energies of  $\text{Ta}_2\text{O}_5$ , TaON, and  $\text{Ta}_3\text{N}_5$  by Electrochemical Measurement and UPS**

method	material	$E_{\text{BG}}$	$E_{\text{F}}$	$E_{\text{VB}}$	$E_{\text{CB}}$	$\Delta E^a$
electrochem.	$\text{Ta}_2\text{O}_5/\text{Ta}$	3.9	-4.23	-7.83	-3.93	
measmt (EC)	TaON/Pt	2.4	N/A	N/A	N/A	0.3 (assumed)
at pH = 0	$\text{Ta}_3\text{N}_5/\text{Ta}$	2.1	-4.44	-6.02	-4.14	
UPS	$\text{Ta}_2\text{O}_5/\text{Ta}$	3.9	-4.45	-7.93	-4.03	-0.42
	TaON/Pt	2.4	-4.41	-6.6	-4.1	-0.21
	$\text{Ta}_3\text{N}_5/\text{Ta}$	2.1	-4.21	-6.02	-3.92	-0.29

<sup>a</sup> Difference between  $E_{\text{CB}}$  and  $E_{\text{F}}$ .

by the two methods for  $\text{Ta}_2\text{O}_5$  and  $\text{Ta}_3\text{N}_5$  are in good agreement. In addition, the band position of  $\text{Ta}_2\text{O}_5$  determined here is consistent with electrochemical potential measurement in the literature.<sup>18</sup>

The difference between  $E_{\text{F}}$  and  $E_{\text{CB}}$  can be determined experimentally by UPS.  $E_{\text{F}}$  is assumed to occur at the same position as for Au deposited on the samples. Thus, the difference between  $E_{\text{F}}$  and  $E_{\text{CB}}$  can be determined directly. The results indicate that the assumption made for electrochemical analysis, the difference being  $-0.3$  V, is reasonable.

Although the  $E_{\text{CB}}$  values for  $\text{Ta}_2\text{O}_5$ , TaON, and  $\text{Ta}_3\text{N}_5$  are similar, the  $E_{\text{VB}}$  values vary significantly between these materials as shown in Figure 13. The  $E_{\text{VB}}$  values of TaON and  $\text{Ta}_3\text{N}_5$  are at higher potential energies than that of  $\text{Ta}_2\text{O}_5$ .

The change in band positions obtained in this work is reasonably explained by density function theory (DFT) calculations.<sup>19</sup> DFT calculations revealed that a structure at  $-9$  eV in UPS spectrum was attributed to O2p orbitals for TaON and  $\text{Ta}_2\text{O}_5$ . But it was suggested that some structures at around  $-8$  eV were attributable to N2p orbitals for  $\text{Ta}_3\text{N}_5$ . The calculations of electronic band structures indicated that the valence bands of  $\text{Ta}_2\text{O}_5$ , TaON, and  $\text{Ta}_3\text{N}_5$  consist mainly of O2p, O2p + N2p, and N2p orbitals, respectively. The conduction bands consist of Ta5d orbitals for all three materials.<sup>19</sup> The  $E_{\text{CB}}$  values, however, vary slightly among three samples, as shown in Figure 13. It might occur due to the difference of the crystal structures. But it is difficult to examine the detail of the difference at the present stage because the errors of UPS and electrochemical methods in our experiments are estimated to be 0.1–0.2 eV. Thus, the band gaps of an oxynitride or nitride are smaller than the corresponding oxide. These band structures are shown schematically in Figure 14.

It should be noted that all the materials studied in this work have the potential for overall water splitting. Of particular interest are TaON ( $\lambda \leq 520$  nm) and  $\text{Ta}_3\text{N}_5$  ( $\lambda \leq 600$  nm), which have good absorption in the visible regime. Moreover, previous investigations of photocatalytic reactions by the present au-

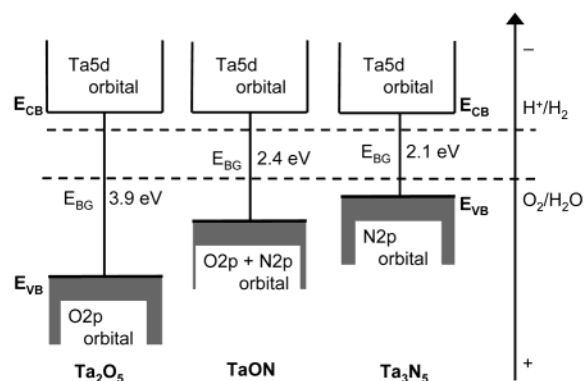


Figure 14. Schematic band structures of Ta<sub>2</sub>O<sub>5</sub>, TaON, and Ta<sub>3</sub>N<sub>5</sub>.

thors<sup>5,6</sup> demonstrated that TaON and Ta<sub>3</sub>N<sub>5</sub> are essentially stable during photooxidation and photoreduction of water. These results indicate that this oxynitride and nitride are potential photocatalysts for overall water splitting with good visible light absorption.

## 5. Conclusion

The band gap positions of Ta<sub>2</sub>O<sub>5</sub>, TaON, and Ta<sub>3</sub>N<sub>5</sub> were determined by electrochemical analysis and UPS. The conduction band positions of Ta<sub>2</sub>O<sub>5</sub>, TaON, and Ta<sub>3</sub>N<sub>5</sub> were found to be largely similar, whereas the valence band positions vary significantly (Ta<sub>2</sub>O<sub>5</sub> < TaON < Ta<sub>3</sub>N<sub>5</sub>). The change in the band positions is reasonably consistent with the results of DFT calculations. The results indicate that TaON and Ta<sub>3</sub>N<sub>5</sub> are potential photocatalysts for overall water splitting utilizing solar radiation. Moreover, the results of UPS analysis are in good agreement with the electrochemical analysis, demonstrating that the proposed UPS technique is a reliable alternative means of determining the band positions of a wide range of photocatalytic materials.

**Acknowledgment.** We acknowledge the Core Research for Evolutional Science and Technology (CREST) program of the Japan Science and Technology Corp. (JST) for support of this research and thank Dr. T. Kubota of RIKEN for UPS measurements.

## References and Notes

- (1) Domen, K.; Kudo, A.; Ohnishi, T. *J. Catal.* **1986**, *102*, 92.
- (2) Takata, T.; Furumi, Y.; Shinohara, K.; Tanaka, A.; Hara, M.; Kondo, J. N.; Domen, K. *Chem. Mater.* **1997**, *9*, 1063.
- (3) Kudo, A.; Tanaka, K.; Domen, K.; Maruya, K.; Aika, K.; Onishi, T. *J. Catal.* **1988**, *111*, 67.
- (4) Kasahara, A.; Nukumizu, K.; Hitoki, G.; Takata, T.; Kondo, J. N.; Hara, M.; Kobayashi, H.; Domen, K. *J. Phys. Chem. A* **2002**, *106*, 6750.
- (5) Hitoki, G.; Ishikawa, A.; Takata, T.; Kondo, J. N.; Hara, M.; Domen, K. *Chem. Lett.* **2002**, 736.
- (6) Hitoki, G.; Takata, T.; Kondo, J. N.; Hara, M.; Kobayashi, H.; Domen, K. *Chem. Commun.*, **2002**, 1698.
- (7) Trasatti, S. *Pure Appl. Chem.* **1986**, *58*, 955.
- (8) Swisher, J. H.; Read, M. H. *Metall. Trans.* **1972**, *3*, 489.
- (9) Koura, N.; Tsukamoto, T.; Shoji, H.; Hotta, T. *Jpn. J. Appl. Phys.* **1995**, *34*, 1643.
- (10) Matsumoto, Y.; Funatsu, A.; Matsuo, D.; Unal, U. *J. Phys. Chem. B* **2001**, *105*, 10893.
- (11) Brese, N. E. *Acta Crystallogr., Sect. C* **1991**, *47*, 2291.
- (12) Armytage, B.; Fender, B. E. F. *Acta Crystallogr., Sect. B* **1974**, *30*, 809.
- (13) Kerrec, O.; Devilliers, D.; Groult, H.; Marcus, P. *Mater. Sci. Eng.* **1998**, *B55*, 134.
- (14) Huygens, I. M.; Strubbe, K.; Gomes, W. P. *J. Electrochem. Soc.* **2000**, *147*, 1797.
- (15) Hufner, S. *Photoelectron Spectroscopy: Principles and Applications*; Springer Verlag: 1995.
- (16) Matsumoto, Y.; Omae, K.; Watanabe, I.; Sato, E. *J. Electrochem. Soc.* **1986**, *133*, 711.
- (17) Matsumoto, Y. *J. Solid State Chem.* **1996**, *126*, 227.
- (18) Halouani, F. E.; Deschanvres, A. *Mater. Res. Bull.* **1982**, *17*, 1045.
- (19) Fang, C. M.; Orhan, E.; Wijs, G. A.; Hintzen, H. T.; Groot, R. A.; Marchand, R.; Saillard, J.-Y.; With, G. *J. Mater. Chem.* **2001**, *11*, 1248.